The 8th International Supercritical CO_2 Power Cycles Symposium
February 27 – 29, 2024, San Antonio, Texas
Paper #78

Analysis and optimization of the recompression cycle with high-temperature recuperator bypass for concentrating solar power applications

Taylor Brown
Thermal Systems R&D Group
National Renewable Energy Laboratory
Golden, CO, USA

Ty Neises
Thermal Systems R&D Group
National Renewable Energy Laboratory
Golden, CO, USA

Taylor is a researcher in the Thermal Systems group at NREL. His research focuses on modeling concentrating solar power systems and sCO_2 power cycles. Taylor's work includes modeling linear Fresnel and parabolic trough systems for NREL's System Advisor Model.

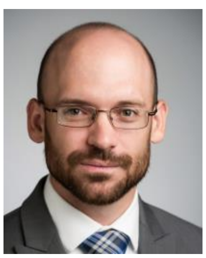

Ty is a senior researcher in the Thermal Systems group at NREL where he focuses on techno-economic analysis of thermal energy systems. Ty leads development of thermal technology models in NREL's System Advisor Model (SAM). Ty's sCO2 research focuses on developing models to understand the integration of sCO2 cycles with solar thermal and thermal energy storage.

ABSTRACT

This work analyzes the sCO2 recompression with high temperature recuperator (HTR) bypass power cycle for use in concentrating solar power (CSP) systems. CSP operation differs from other thermal power plants in that CSP must balance between maximizing the heat transfer fluid (HTF) temperature difference and maximizing the cycle thermal efficiency, which typically are inversely related. Large HTF temperature differences reduce the size and cost of thermal energy storage (TES), improve the solar receiver efficiency, and require lower mass flow rates that reduce pumping power required to elevate the HTF to the receiver. The recompression cycle with HTR bypass potentially offers improved thermal efficiency with larger HTF temperature differences as compared to the recompression cycle, and it has fewer turbomachinery components than the partial cooling cycle. The recompression with HTR bypass cycle adds a second lower temperature primary heat exchanger which transfers heat from the HTF to the fraction of sCO2 flow that bypasses the HTR. We developed a model to compare the recompression with HTR bypass cycle to the recompression and partial cooling cycles. A sweep of design parameters including bypass fraction, recompression fraction, recuperator

conductance, and pressure ratio is used to form a pareto-optimal front with the cycle thermal efficiency and HTF temperature difference as objectives. An optimization routine has also been developed to find optimal design point parameters for a target HTF temperature difference. The performance of the recompression with HTR bypass cycle is compared with recompression and partial cooling cycles.

INTRODUCTION

Supercritical carbon dioxide power cycles are being studied as an alternative to steam Rankine cycles for their potential higher thermal efficiency and compact turbomachinery. Applications such as waste heat recovery, coal power plants, and concentrating solar power (CSP) systems are possible use case scenarios for sCO_2 power cycles. CSP systems are different than waste heat and coal power plants because the heat transfer fluid (HTF) temperature difference influences the CSP system design, cost, and performance. Large HTF temperature differences allow the field to use less mass flow, because more energy is absorbed relative to mass flow rate. With less mass flow, less storage mass is required, saving size and cost. In addition, the lower average temperature of the HTF across the receiver decreases receiver thermal losses.

Past studies show that larger HTF temperature differences passing heat into the power cycle result in lower efficiency of the cycle [1]. This is because higher efficiency cycles recuperate more heat back into the cycle, resulting in lower temperature differences for the HTF. For CSP applications, there is a balance between the benefit of large HTF temperature differences and the decreased thermal efficiency. Multiple cycle configurations have been studied, including the simple, recompression, and partial cooling cycles. Work by Neises and Turchi [1] show partial cooling cycles have the best combination of thermal efficiency and HTF temperature delta to minimize the LCOE of a molten salt power tower plant. The partial cooling cycle, however, includes three compressors, compared to the two compressors of the recompression cycle. The additional compressor represents an increase in cost and complexity of the system. Neises and Turchi also investigated how the recuperator design affects the levelized cost of energy (LCOE) for the full CSP system and determined that it is not always optimal to maximize recuperator conductance when optimizing for LCOE.

The recompression with HTR bypass (RC-BP) cycle maintains the relative simplicity of the recompression cycle and adds a bypass to the HTR, having a portion of flow pass through a bypass HTF heat exchanger. The desired effect is to absorb additional heat from the HTF, further reducing its outlet temperature. The portion of flow that bypasses the high temperature recuperator is controlled by the bypass fraction. A schematic of the cycle is shown in Figure 1.

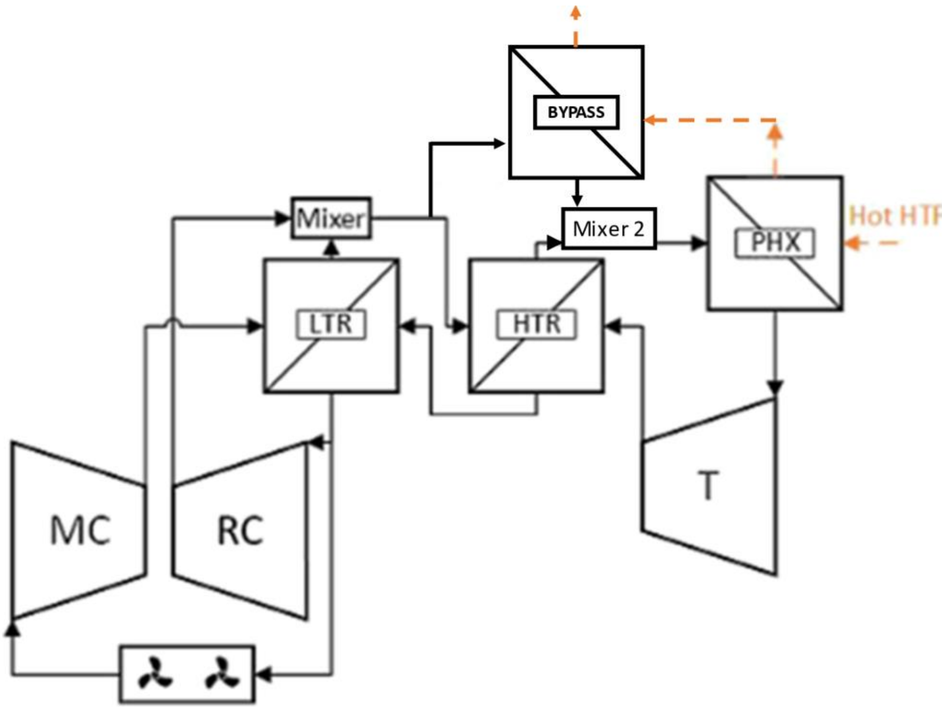

Figure 1. Recompression with HTR bypass (RC-BP) schematic.

Alfani et al. 2019 [2] studied the RC-BP cycle for a 5.21 MW waste heat application. The optimal cycle had a 27% thermal efficiency and an HTF temperature difference of 335.94 °C. The HTF was modeled to represent a flue gas stream from a combustion process. Alfani et al. 2021 [3] further modeled five different cycle configurations for waste heat and concluded the RC-BP cycle was not as effective at utilizing waste heat as non-recompression based configurations.

The sCO_2 flex project [4], funded by the European Union's Horizon 2020 research and innovation program, studied incorporating sCO_2 power cycles into coal power plants. Many cycle configurations were studied, including variations of recompression, partial cooling, pre-compression, turbine split-flow, and preheating cycles. The RC-BP cycle was modeled and produced a 46.13% thermal efficiency for a 25 MW system. The project, however, ultimately chose the recompression with double reheat, partial cooling with double reheat, and pre-compression cycles as the most optimal cycle designs [5].

Moullec et al. [6] modeled multiple cycle configurations to retrofit a 10 MW CSP plant. The RC-BP model had a 34.4% efficiency with a 240 °C HTF temperature difference. However, the recompression with intercooling and preheating was selected as the optimal cycle design, with a 35.6% efficiency and 240 °C HTF temperature difference.

The relationship between the bypass fraction and cycle performance is not clear, as well as how the effect of bypass fraction compares to the effect of decreasing the recuperator total conductance in the cycle. This work explores these relationships.

METHODOLOGY

Design Point Model

This model of the RC-BP cycle is based on NREL's recompression cycle model used in prior analyses [1], with a few added parameters to encapsulate the bypass behavior. The model designs the cycle for a user defined net power output, using user provided inputs such as turbomachinery efficiencies, total recuperator conductance, HTF inlet temperature, maximum sCO_2 pressure, and approach temperatures to the primary heat exchanger and air cooler. The cycle pressure ratio, recompression fraction, and allocation of conductance between the two recuperators can either be set by the user or optimized by the model, which is discussed in more detail in the following sections.

The HTR bypass adds a bypass fraction to the model, which controls the fraction of flow that bypasses the HTR and passes through the bypass heat exchanger. The user can either define the bypass fraction, or have the model optimize the value to target an HTF outlet temperature defined by the user. Additionally, we set the sCO_2 temperature difference between the flows entering the mixer that joins the bypass and HTR flow to 0 °C for this study.

Design Point Model Validation

We compared the recompression with HTR bypass model with multiple cases in literature that contain detailed performance results. The pressure loss in heat exchangers was calculated as a function of total pressure and was based on data from each case in literature. Table 1 shows the comparison of four cases, with key inputs and results.

Table 1. Design point model comparison with literature.

	sCO_2 Flex 2018 [4] **(coal)**		**Alfani 2020** [7] **(coal)**		**Moullec 2019** [6] **(CSP)**		**Alfani 2019** [2] **(waste heat)**	
	Paper	**Model**	**Paper**	**Model**	**Paper**	**Model**	**Paper**	**Model**
W design (MW)	25	25	108.428	108.428	10.01	10.01	5.863	5.863
Q PHX (MW)	44.8	43.79	189.21	189.12	-	-	15.364	15.37
Q BP (MW)	9.42	9.22	44.02	44.38	-	-	3.95	3.95
W t (MW)	36.82	36.58	159.54	159.41	-	-	10.25	10.23
W mc (MW)	4.71	4.58	20.48	20.35	-	-	1.48	1.47
W rc (MW)	7.12	6.99	30.64	30.63	-	-	2.9	2.89
Total HX Pressure Loss (MPa)	-	-	0.631	0.655	-	-	0.443	0.443
sCO2 mdot (kg/s)	239	232.6	1041.54	1040.64	162.94	163.02	140.17	138.98
HTF Outlet Temp (C)	-	568.12	-	460.98	290	291.19	214.06	212.31
Thermal Eff. (%)	46.13	47.16	46.49	46.43	34.4	34.3	30.35	30.41

As is shown from the comparison, the model shows close agreement with the cases in literature. The largest discrepancy is from the sCO_2 flex project [4] which is the earliest paper used for comparison and as such may be missing detail that is captured in later papers. The T-S diagram of the Alfani 2020 case [7] is shown in Figure 2.

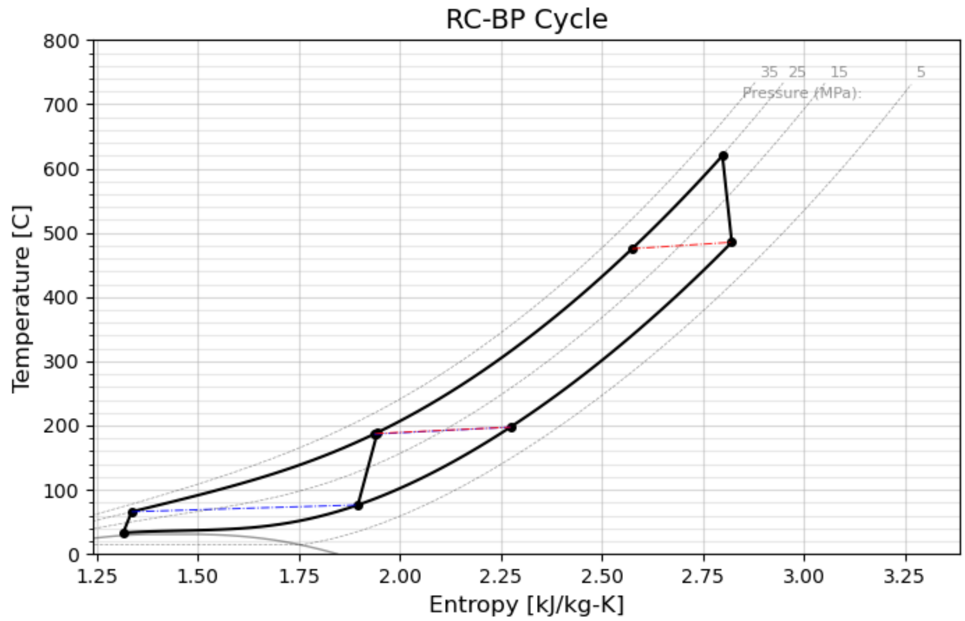

Figure 2. T-S Diagram from Alfani 2020 case [7]

Optimization

The addition of the HTR bypass to the recompression cycle requires the optimization to behave differently than the simple, recompression, or partial cooling cycles. Rather than optimizing for efficiency only, which would prevent the bypass fraction from opening, the optimizer must optimize for two objectives: thermal efficiency and HTF temperature difference. For this model, the user defines a target HTF outlet temperature, and the optimizer designs the system to maximize thermal efficiency while hitting the target outlet temperature. This is accomplished by setting the objective value to thermal efficiency and penalizing the objective proportionally to the difference between the actual outlet temperature and the target. This ensures that the cycle will hit the target temperature, if possible, and then optimize for efficiency.

The bypass introduces nonlinear behavior, and the optimization routine involves two nested nonlinear optimizations as a result. NLopt [8–10] is used as the nonlinear optimizer. The outer optimization chooses bypass fraction, and the inner loop optimizes pressure ratio, recompression fraction, and allocation of total recuperator conductance between the low- and high- temperature recuperators. This process is shown in Figure 3.

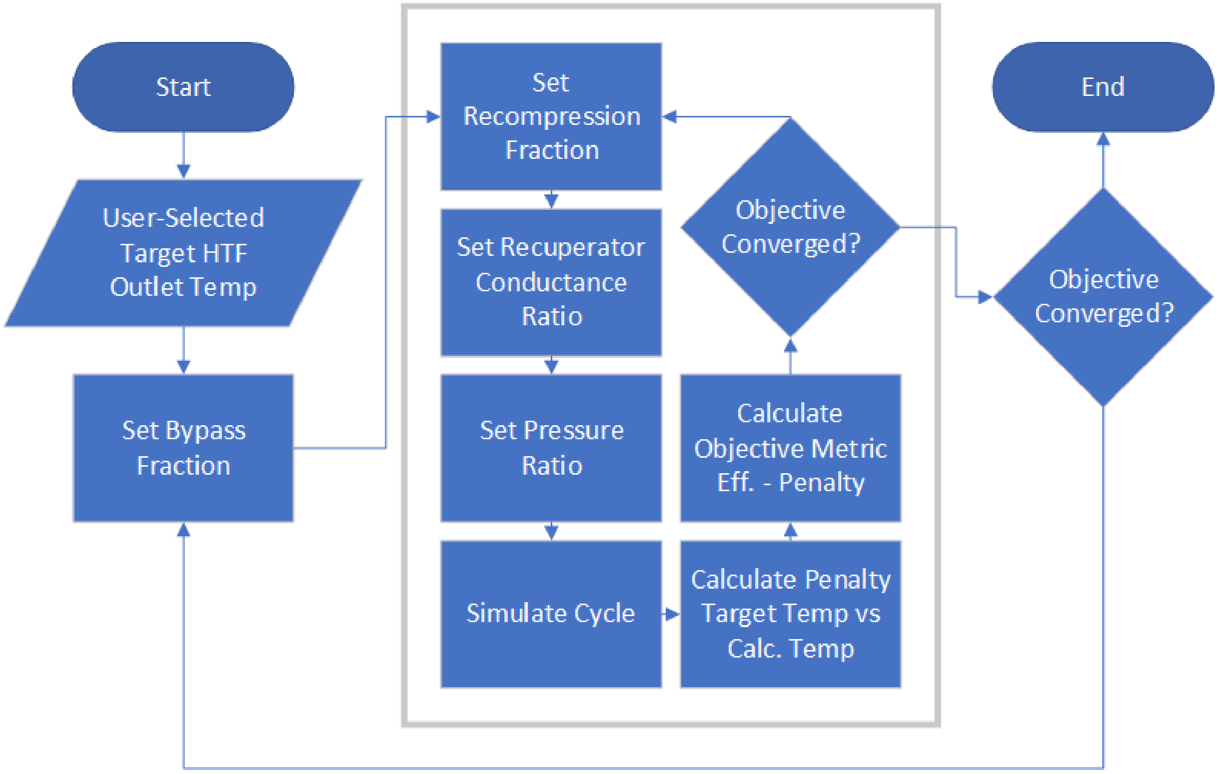

Figure 3. Optimization flow chart.

Optimization Validation

To evaluate the success of our optimization routine in this non-linear problem, we simulated a large parametric sweep of design parameters (bypass fraction, recompression fraction, pressure ratio, and conductance allocation between the two recuperators) to form the design space of solutions. The sweep divided each parameter into 20 values, which resulted in 160,000 total runs. The design variables and their respective ranges are shown in Table 2. From this, a pareto front targeting HTF outlet temperature and thermal efficiency was derived, representing a collection of optimal case designs. To validate optimizer results, we ran a series of cases to find optimal solutions for a range of outlet temperatures. The fixed cycle parameters were based on the 100 MW Alfani coal power plant cycle design [7] and key parameters are shown in Table 3. Figure 4 shows a comparison between the pareto front and optimizer solutions.

Table 2. Design variables.

Design Variable	**Unit**	**Range**
Bypass Fraction		0-1
Recompression Fraction		0-1
Minimum Pressure	MPa	7-12
Recuperator Conductance Split Fraction		0-1

Table 3. Key cycle parameters.

Parameter	Unit	Value
Net Power	MWe	100
HTF Inlet Temperature	C	640
PHX Inlet Approach Temperature	C	20
Ambient Temperature	C	25
Air Cooler Approach Temperature	C	8
Turbine Isentropic Efficiency	%	89.8
Main Compressor Polytropic Efficiency	%	77.7
Recompressor Polytropic Efficiency	%	76.7
Max Pressure	MPa	25
Air Cooler Parasitic Power	MWe	0.87805
Total Recuperator Conductance	MW/K	36.85

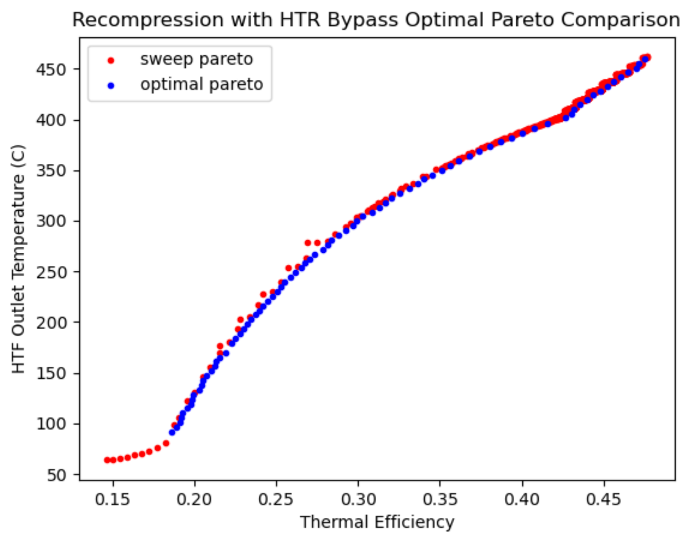

Figure 4. Optimizer comparison with pareto front.

As is shown, the optimization routine successfully finds optimal solutions over the range of target HTF outlet temperatures.

RESULTS AND DISCUSSION

The RC-BP cycle was compared with the simple, recompression, and partial cooling cycles by forming pareto fronts for each configuration. A large parametric sweep of each design variable was created to visualize the design space, and the pareto fronts were derived from the result. Each configuration was parameterized using the variables and ranges in Table 2, except the partial cooling cycle, which used a minimum pressure range from 3 to 12 MPa, because of its inherently lower minimum pressure. Because of a limitation in the model, the partial cooling cycle recompressor used an isentropic efficiency, rather than polytropic, set to 73.9%, calculated using estimated pressure and temperature values at the recompressor inlet and outlet. Importantly, the total conductance of the recuperators was set constant, and the ratio of LTR and HTR conductance was modified in the sweep. Figure 5 shows data from each of the four sweeps and the corresponding pareto front. The pareto fronts are extracted and compared in Figure 6.

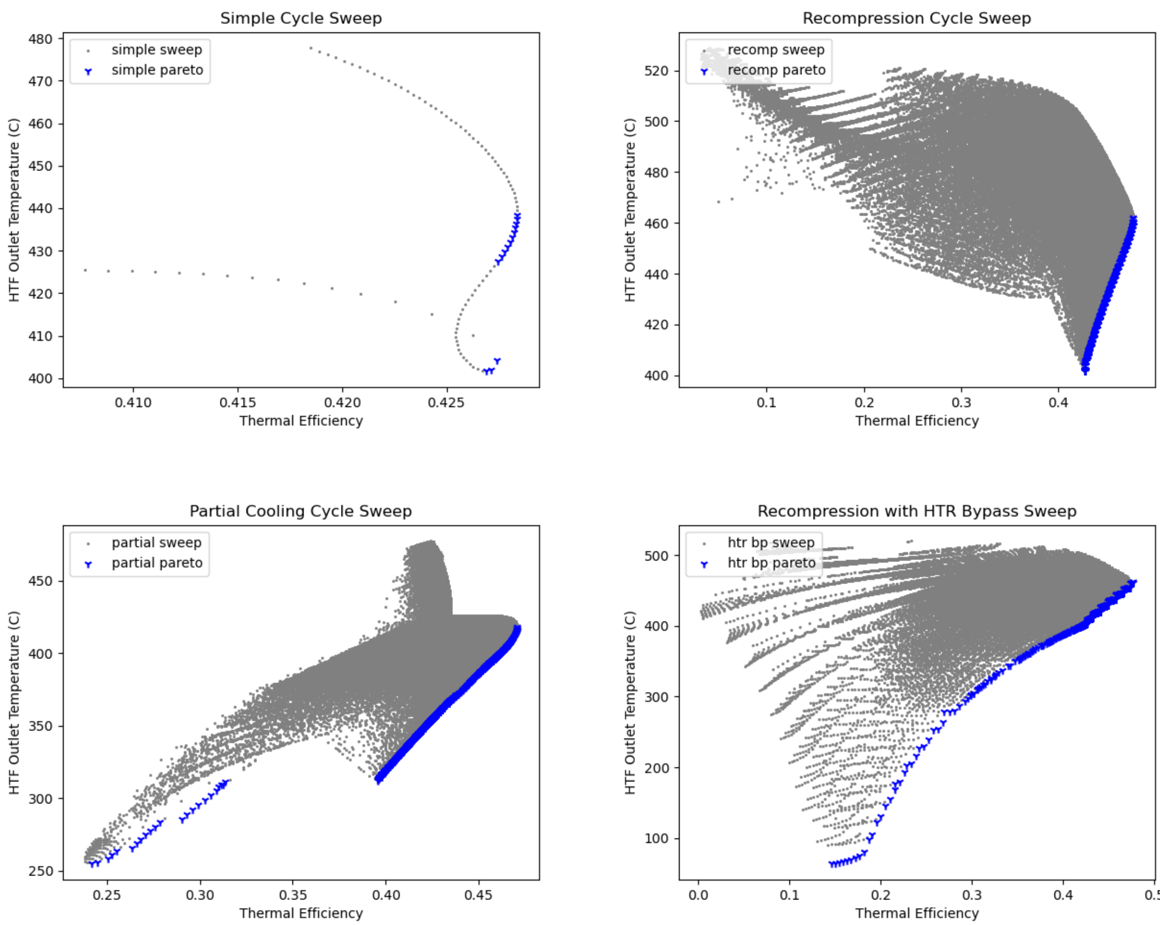

Figure 5. sCO_2 cycle parameter sweeps with pareto fronts.

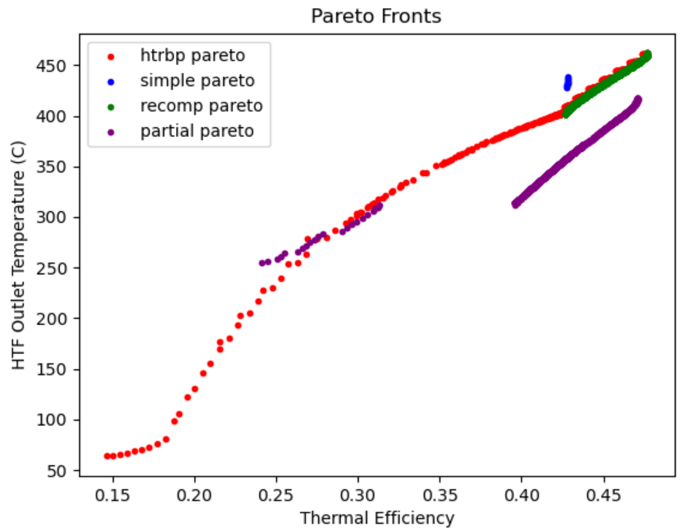

Figure 6. Pareto front comparison.

From Figure 6, it is clear the partial cooling cycle has the best combination of thermal efficiency and HTF temperature difference. The gap in efficiency around 310 °C is due to the partial cooling cycle hitting the lower pressure limit. The recompression and RC-BP cycles have the same performance for cases with low HTF temperature difference (178 °C – 238 °C), but RC-BP cycle can reach lower outlet temperatures by opening the bypass fraction. As is shown later, the recompression cycle can hit lower HTF outlet temperatures but must modify the recuperator total conductance. The simple cycle, as expected, performs worse than the others, with a small domain space because of the lack of free design parameters.

The results suggest that the RC-BP cycle is less efficient than the partial cooling cycle but capable of reaching lower target HTF temperatures than the recompression cycle. However, the total conductance of the recuperators was set as a constant (36.85 MW/K) for each cycle, which is not necessary when designing a system. It is possible that a decreased total recuperator conductance results in a higher efficiency cycle at a given HTF temperature difference. Therefore, we analyzed the performance of each configuration with varying total recuperator conductances.

We simulated each configuration with a range of total recuperator conductances from 0.1 to 50 MW/K, with all other design variables optimized for efficiency. The recompression with HTR bypass cycle followed the same method, with the addition of a sweep of target HTF outlet temperatures. These simulations produced a new pareto front, this time created by the varied total conductance. Figure 7 shows each of these pareto fronts.

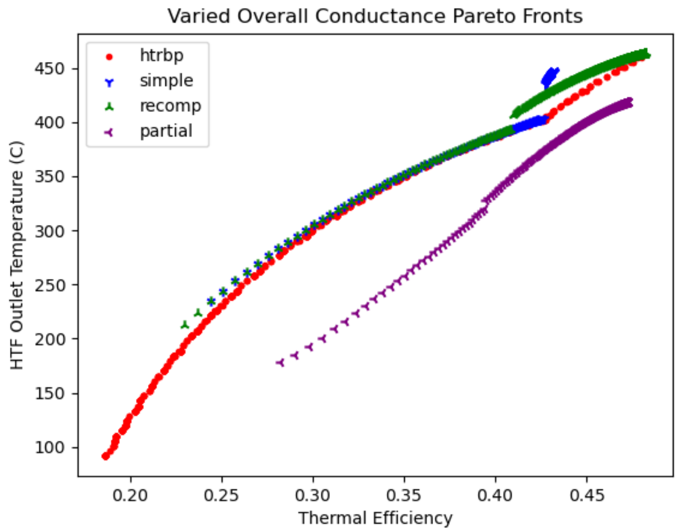

Figure 7. sCO_2 cycle performance comparison with varied total recuperator conductance

As is shown in Figure 7, the cycles can hit a wider range of outlet HTF temperatures by decreasing the total recuperator conductance. This is due to the cycles absorbing more heat from the HTF, because less heat was recuperated back into the low-pressure side of the cycle. The decrease in recuperated heat penalizes thermal efficiency; however, when optimizing for HTF temperature difference and efficiency, low recuperator conductances can provide optimal results.

The recompression cycle performance becomes much closer to the performance with the HTR bypass when factoring in varied conductances. The cycle can hit the same HTF outlet temperatures at nearly the same efficiency as the HTR bypass cycle. As the target outlet temperature decreases, the HTR bypass cycle becomes more efficient relative to the recompression cycle, and the maximum advantage in efficiency is 0.9 percentage points at an outlet temperature of 212 °C.

To further analyze the relationship of the recompression cycle with and without the HTR bypass, we parametrically varied the bypass fraction of an optimal recompression solution, shown in Table 4, with all other parameters set constant, shown in Table 3. This shows the direct effect of opening the bypass fraction, shown on Figure 8. For comparison, the pareto front from the recompression cycle design variable sweep is included in the plot.

Table 4. Optimal recompression cycle design parameters.

Design Variable	Unit	Value
Recompression Fraction		0.343
Minimum Pressure	MPa	7.937
LTR Conductance	MW/K	21.954
HTR Conductance	MW/K	14.898

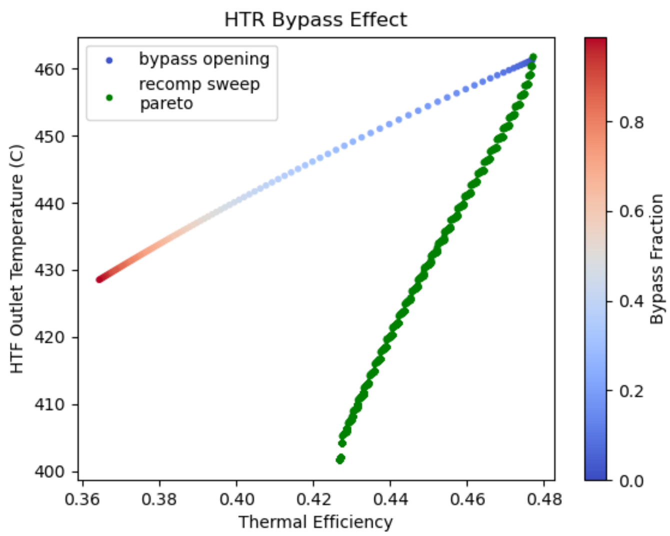

Figure 8. Comparison of recompression cycle pareto front and directly opening bypass fraction.

The results show that opening the bypass fraction decreases the HTF outlet temperature, but at the expense of thermal efficiency. Alternatively, modifying other design parameters, such as recompression fraction, recuperator conductance ratio, and pressure ratio has a larger effect on HTF outlet temperatures, with higher efficiency.

CONCLUSIONS

Overall, the addition of the HTR bypass does not affect HTF temperature difference to the same extent as other cycle parameters but does show improved efficiencies at large temperature differences compared to the recompression cycle. Varying total recuperator conductance lets the cycles reach lower HTF outlet temperatures, with a sacrifice of efficiency.

In the future, we plan on using cycle cost and CSP system models to further compare the performance of the RC-BP cycle to the recompression and partial cooling cycles. Additionally, we will investigate different design parameters, including HTF inlet temperatures, and the temperature difference at the second mixer.

REFERENCES

[1] Neises, T., and Turchi, C., 2019, “Supercritical Carbon Dioxide Power Cycle Design and Configuration Optimization to Minimize Levelized Cost of Energy of Molten Salt Power Towers Operating at 650 °C,” Solar Energy, **181**, pp. 27–36.

[2] Alfani, D., Astolfi, M., Binotti, M., Macchi, E., and Silva, P., 2019, “OPTIMIZATION OF THE PART-LOAD OPERATION STRATEGY OF SCO2 POWER PLANTS.”

[3] Alfani, D., Binotti, M., Macchi, E., Silva, P., and Astolfi, M., 2021, “SCO2 Power Plants for Waste Heat Recovery: Design Optimization and Part-Load Operation Strategies,” Applied Thermal Engineering, **195**, p. 117013.

[4] Mecheri, M., 2018, *D1.1 - SCO2 Brayton Cycle Architecture and Components' Specifications*.

[5] Mecheri, M., and Bedogni, S., 2018, *D1.3 - Report on the Selected Cycle Architecture*.

[6] Le Moullec, Y., Qi, Z., Zhang, J., Zhou, P., Yang, Z., Wang, X., Chen, W., and Wang, S., 2019, “Shouhang-EDF 10MWe Supercritical CO2 Cycle + CSP Demonstration Project,” Conference Proceedings of the European sCO2 Conference3rd European Conference on Supercritical CO2 (sCO2) Power Systems 2019: 19th-20th September 2019, p. 138.

[7] Alfani, D., Astolfi, M., Binotti, M., and Silva, P., 2020, “Part Load Strategy Definition and Annual Simulation for Small Size SCO2 Based Pulverized Coal Power Plant.”

[8] Johnson, S. G., “The NLopt Nonlinear-Optimization Package.”

[9] Rowan, T., 1990, “Functional Stability Analysis of Numerical Algorithms,” Ph.D. Thesis, University of Texas at Austin.

[10] Jones, D. R., Perttunen, C. D., and Stuckman, B. E., 1993, “Lipschitzian Optimization without the Lipschitz Constant,” J Optim Theory Appl, **79**(1), pp. 157–181.

ACKNOWLEDGEMENTS

This work was authored by the National Renewable Energy Laboratory, operated by Alliance for Sustainable Energy, LLC, for the U.S. Department of Energy (DOE) under Contract No. DE-AC36-08GO28308. Funding provided by the U.S. Department of Energy Office of Energy Efficiency and Renewable Energy Solar Energy Technologies Office. The views expressed in the article do not necessarily represent the views of the DOE or the U.S. Government. The U.S. Government retains and the publisher, by accepting the article for publication, acknowledges that the U.S. Government retains a nonexclusive, paid-up, irrevocable, worldwide license to publish or reproduce the published form of this work, or allow others to do so, for U.S. Government purposes.